J Nanostruct 15(4): 1994-2004, Autumn 2025

RESEARCH PAPER

Characterization of Niobium Carbide Film Deposited on Ti-6Al-7Nb Alloy by Low Temperature Plasma Glow Discharge

Haitham T. Al Qaysi [1], Thair L. Al Zubaidy [2], Thekra I. Hamad [1]*

[1] *Department of Prosthodontics, College of Dentistry, University of Baghdad, Baghdad, Iraq*

[2] *Department of Prosthetic Dental Techniques, College of Health and Medical Techniques, AlEsraa University, Baghdad, Iraq*

ARTICLE INFO

Article History:
Received 19 June 2025
Accepted 29 September 2025
Published 01 October 2025

Keywords:
Contact angle
Niobium carbide
Plasma glow discharge
Roughness
Thin films

ABSTRACT

Niobium carbide thin films were successfully deposited on a Ti-6Al-7Nb substrate using a low-temperature plasma glow discharge method, employing argon gas and C_2H_2 as the carbon source. Three different deposition times were employed to apply the coatings: Group 1 had a deposition period of two hours, Group 2 had a deposition period of four hours, and Group 3 had a deposition period of six hours. The phase composition, microstructure, surface morphology, roughness, and wettability of the films were examined as a function of deposition time. Various phases of niobium carbide were observed, with the sputter deposition process resulting in a nanocomposite structure composed of a nanocrystalline and often substoichiometric niobium carbide phase, along with an amorphous carbon phase. The microstructure of the deposited layers exhibited consistency and homogeneity. The SEM images displayed an organized morphology characterized by the material's agglomerating feature on a striated texture. The coated samples exhibited a more prominent and rougher surface, with noticeable projections. Furthermore, the water contact angle value decreased from approximately 63° for the untreated Ti-6Al-7Nb surface to around 44° for the coated samples.

How to cite this article
Al Qaysi H., Al Zubaidy T., Hamad T. Characterization of Niobium Carbide Film Deposited on Ti-6Al-7Nb Alloy by Low Temperature Plasma Glow Discharge. J Nanostruct, 2025; 15(4):1994-2004. DOI:10.22052/JNS.2025.04.045

INTRODUCTION

Ti-6Al-7Nb stands as a titanium-based alloy renowned for its potential in bone-contact applications, particularly within orthopedic and dental implant contexts. Distinguished by its composition of titanium, aluminum, and niobium, this alloy has been a focal point of extensive research [1]. Its mechanical properties, corrosion resistance, and biological characteristics have attracted significant attention, surpassing those of pure titanium (CpTi). This superiority can be attributed to the alloy's lack of vanadium. [2]. Notably, the inclusion of niobium in place of vanadium within various titanium-based alloys has led to the stabilization of the β phase and a substantial enhancement in biocompatibility [3]. This alloy holds great promise for diverse biomedical applications.

The initial stage of cell attachment to the implant surface plays a crucial role in the overall bone regeneration process. Consequently, numerous studies have focused on developing biomaterials with favorable surface properties that enhance cell adhesion. Surface roughness [4], topography [5,6], wettability [7], zeta potential [8], biomaterial porosity [9], and the application

* *Corresponding Author Email: htadental1979@gmail.com*

of specific bioactive compounds have all been observed to influence osteoblast cell adhesion [10].

Biomaterials, particularly metallic ones, must possess well-defined surface properties to effectively function in demanding biological environments and achieve appropriate levels of implant osseointegration with bone tissue [11]. Ti-6Al-7Nb holds promise for constructing lightweight and durable osseointegration devices due to its low specific weight, which makes it exceptionally light compared to other metal alloys. Its excellent corrosion resistance, coupled with an elastic modulus approximating that of human bone, enables improved load distribution [12]. While studies have demonstrated these properties in Ti-6Al-7Nb alloy, surface optimization is still necessary to develop a surface topography that promotes cell proliferation, adequate surface roughness for enhanced protein adsorption, and ultimately improved cell viability.

The low temperature plasma glow discharge technique offers a means of treating metallic biomaterial surfaces without significantly altering the substrate's microstructure [13,14]. This method allows for precise control over the growth of thin coatings, including their structure and chemical composition, thus influencing their characteristics. Moreover, it enables surface treatment of complex-shaped components [15].

Niobium carbide (NbC) has garnered significant attention in the field of dental implant materials due to its exceptional combination of properties. These include notable chemical stability [16], high hardness [17], resistance to wear and corrosion, and acceptable biocompatibility. Recent research has explored the deposition of NbC films on 316L stainless steel using a non-reactive configuration, revealing promising osteogenic potential and protective qualities. These findings have positioned NbC as an appealing choice for dental implant applications [18]. Furthermore, studies involving the production of NbC coatings on Ti-6Al-4V through DC magnetron sputtering have demonstrated excellent corrosion resistance and biocompatibility, further underscoring its potential in the field [19].

MATERIALS AND METHODS

Substrate preparation

Ti-6Al-7Nb (ASTM F1295) was utilized as the substrate for all experiments conducted in this investigation. The Ti-6Al-7Nb block was cut into rectangular shapes measuring 12mm by 10mm and with a thickness of 5mm, using a wire cutting machine (Knuth SmartDEM-Germany) [20]. Subsequently, the samples underwent a polishing process using 320, 400, 600, 800, and 1000 grit SiC paper in sequential order, utilizing a polishing machine [21]. To ensure cleanliness, the samples were sonicated twice in acetone, ethanol, and distilled water, each for a duration of 5 minutes, resulting in a total sonication time of 10 minutes. Following the sonication process, the smoothed samples were allowed to air-dry at room temperature for 15 minutes [20,22].

The development of NbC coatings was intended to occur in three distinct groups: Group 1 with a deposition time of 2 hours, Group 2 with a deposition time of 4 hours, and Group 3 with a deposition time of 6 hours.

NbC coating conditions

The NbC films were deposited on Ti-6Al-7Nb samples using a pure Nb target (99.95%) through plasma glow discharge sputtering. The sputtering process was carried out in an Argon gas medium (99.999%) with a reactive gas of C_2H_2 (99.999%). The target was positioned 50 mm away from the substrate holder. Prior to sputtering, the chamber underwent evacuation using a rotary pump and a turbo-molecular pump, reaching a pressure of $1*10^{-4}$ mBar. Before deposition, the substrate was sputtered with Argon gas (25 W) at a pressure of $5*10^{-2}$ mBar for 1 minute. This step was performed to remove the surface oxide layer and any impurities, while preventing additional Nb deposition. The Argon gas was then discontinued, and the chamber pressure was restored to $1*10^{-4}$ mBar. C_2H_2 gas was introduced into the chamber until the pressure stabilized at $1*10^{-2}$ mBar. Following that, Argon gas was introduced to maintain the pressure at $6*10^{-2}$ mBar. The DC voltage was set at 3.7 Kv, and the current was set at 7 mA, resulting in a sputtering energy of 25 Watt, which is the material-dependent ion energy [23].

To ensure a steady-state reaction condition during the deposition process, the working pressure was maintained at $6*10^{-2}$ mBar, which was deemed appropriate for deposition. As the NbC film was intended to be developed via a simple plasma glow discharge, all thin films were deposited at room temperature, and no additional

substrate heating was applied. The deposition times for the coatings were two, four, and six hours.

Film characterization

The phase analysis of the samples was performed using X-Ray Diffraction (XRD) on a SHIMADZU LabX-XRD 6000 Diffractometer equipped with a Cu-Kα X-Ray radiation (λ = 1.540 Å). Diffraction scans were conducted at a tube voltage of 40 kV and a tube current of 30 mA. Each scan was obtained at 2θ values ranging from 20 to 80 degrees, with a step size of 0·05 degrees and a counting duration of 0·6 seconds·

The microstructure was examined using an FEI Inspect F50 field emission-SEM, and the coating thickness was quantified using a FE-SEM on cross-sectional samples. Surface topography and morphology were characterized using the TT-2 AFM model.

Water contact angles were measured utilizing the sessile drop method with a Ramé-Hart Inc. system. Three observations were taken at room temperature using 250µl of water, and the mean values of the advancing angle were calculated.

RESULTS AND DISCUSSION

X-ray diffraction

The X-ray diffraction patterns from both untreated and NbC-treated samples are shown in (Fig. 1). The XRD reflections of the as-received Ti-6Al-7Nb alloy can be indexed with (101), (102), (110), and (112) α titanium orientations, matching the (JCPDS card no. 44-1294). Additionally, (110) and (211) β titanium orientations are observed, matching the (JCPDS card no. 44-1288).

In the XRD pattern of the treated samples, seven peaks are detected, corresponding to the formed

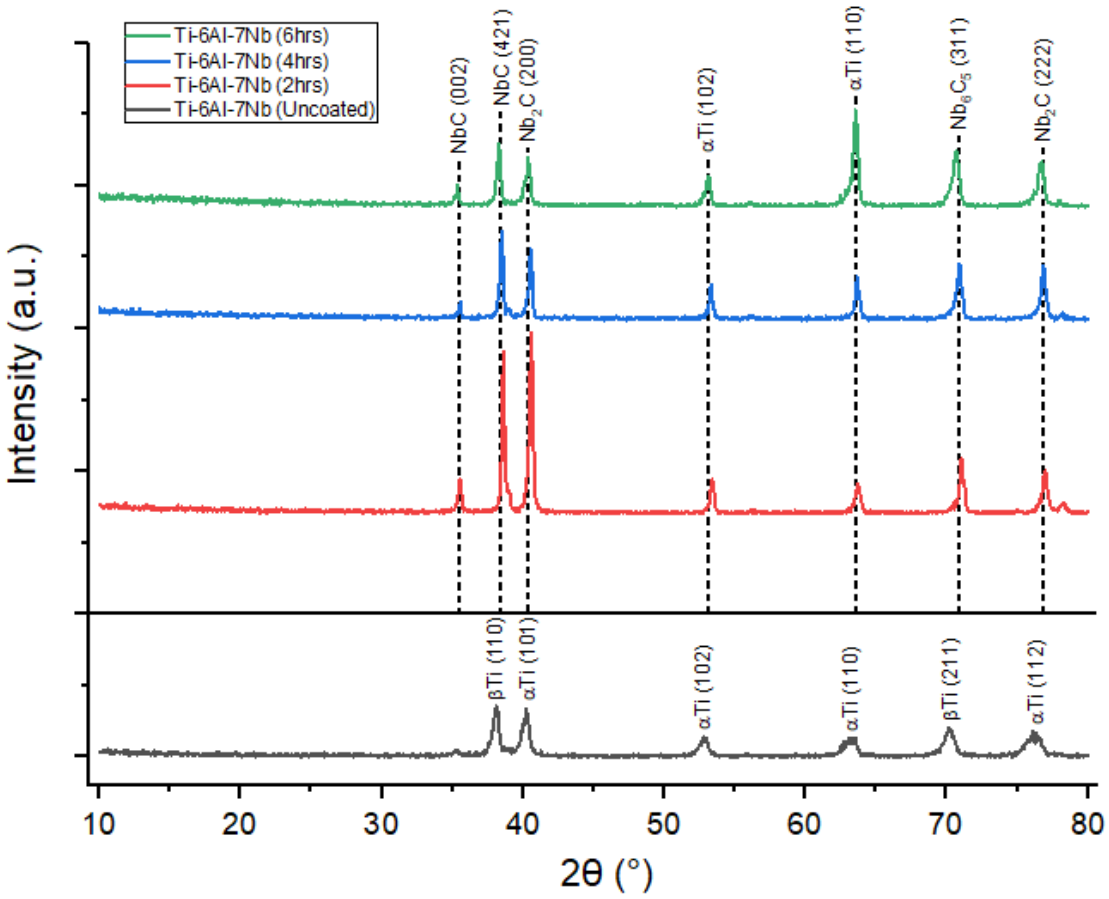

Fig. 1. X-ray diffraction (XRD) spectra for the NbC films with different deposition times: uncoated, 2 hours, 4 hours, and 6 hours.

coating and the underlying substrate material. Two of these peaks are indexed with (002) and (421) NbC orientations, matching the (JCPDS card no. 38-1364). Two other reflections are indexed with (200) and (222) Nb_2C orientations, corresponding to the (JCPDS card no. 19-870). Another peak is indexed with the (311) Nb_6C_5 orientation, corresponding to the (JCPDS card no. 63-503). The remaining two reflections are referenced with (102) and (110) α titanium orientations, matching the (JCPDS card no. 44-1294).

Scanning electron microscopy

The NbC coatings that were deposited for 2, 4, and 6 hours appear in SEM images in (Fig. 2). The microstructure of the deposited layers exhibits consistency and homogeneity. The presence of an organized morphology with an agglomerating feature on a striated texture can be observed. This morphology is a result of the initial treatment process involving grinding and polishing of the sample's surface. Based on the SEM images, the average grain size for the 2-hour deposition time is 0.914 µm, while it increases to 1.33 µm for the 4-hour time and 1.912 µm for the 6-hour time. The grain size shows an increasing trend with longer deposition times.

The thickness of the NbC surface layers formed by the glow discharge procedure is presented in (Table 1).

The discharge treatment creates a continuous

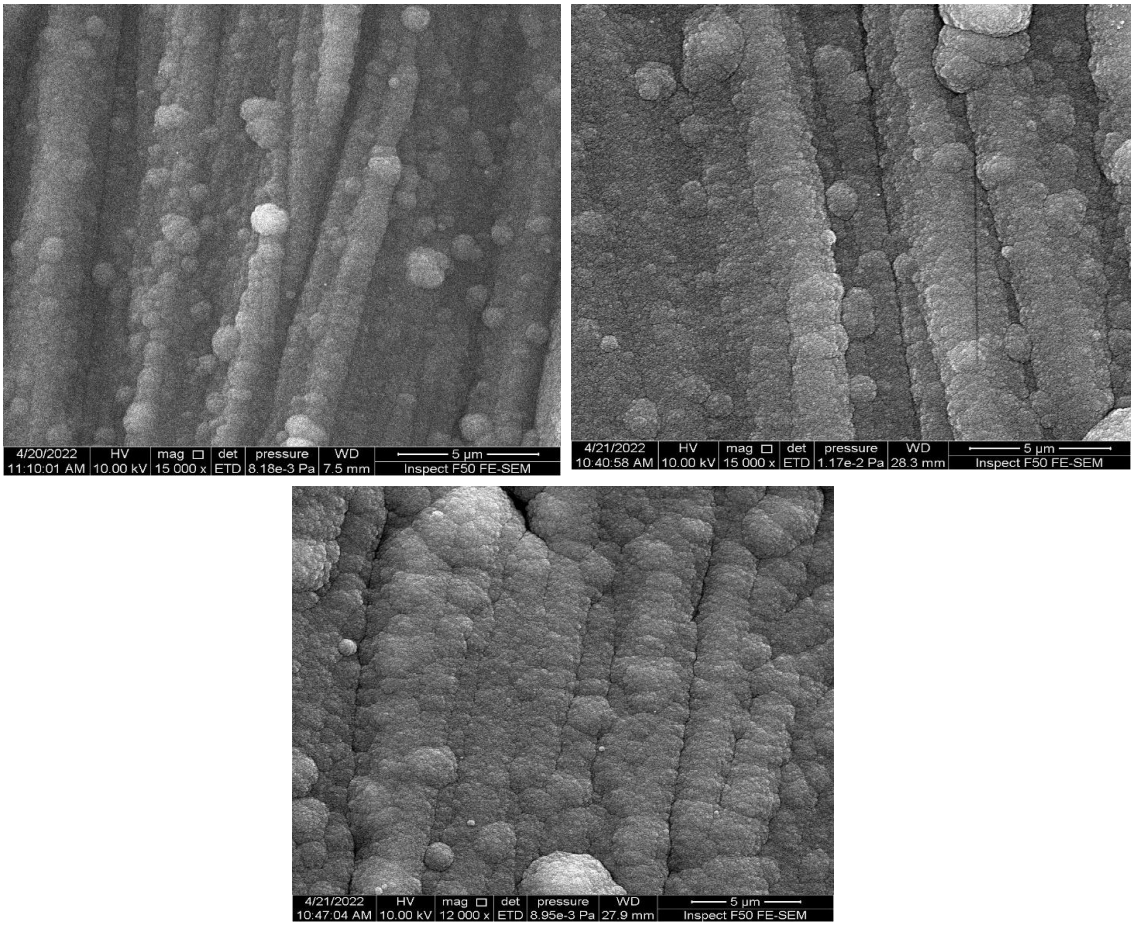

Fig. 2. FE-SEM images of the NbC surface layer with varying deposition times: (a) 2-hour NbC deposited thin film at a magnification of 15,000x, (b) 4-hour NbC deposited thin film at a magnification of 15,000x, and (c) 6-hour NbC deposited thin film at a magnification of 12,000x.

layer of blocky crystallites on the surface, with thickness increasing directly as the sputtering time increases, giving the coating a cumulative effect. The coating thickness of the deposited films, as confirmed by FE-SEM analysis on cross sections of the coated samples, is displayed in (Fig. 3 a, b, & c.).

Atomic force microscopy

The 2D and 3D roughness representations of the uncoated Ti-6Al-7Nb and the NbC films coated for 2 hours, 4 hours, and 6 hours are depicted in (Figs. 4, 5, 6, and 7).

All of the films exhibit nanoscale topographic features, with R_a and R_q values falling within the

Table 1. Mean of the coating thickness measurements for the NbC coated samples.

	2hrs	4hrs	6hrs
NbC coating thickness (µm)	1.452	3.522	6.673
SD	0.253	0.314	0.583
SE	0.126	0.157	0.291

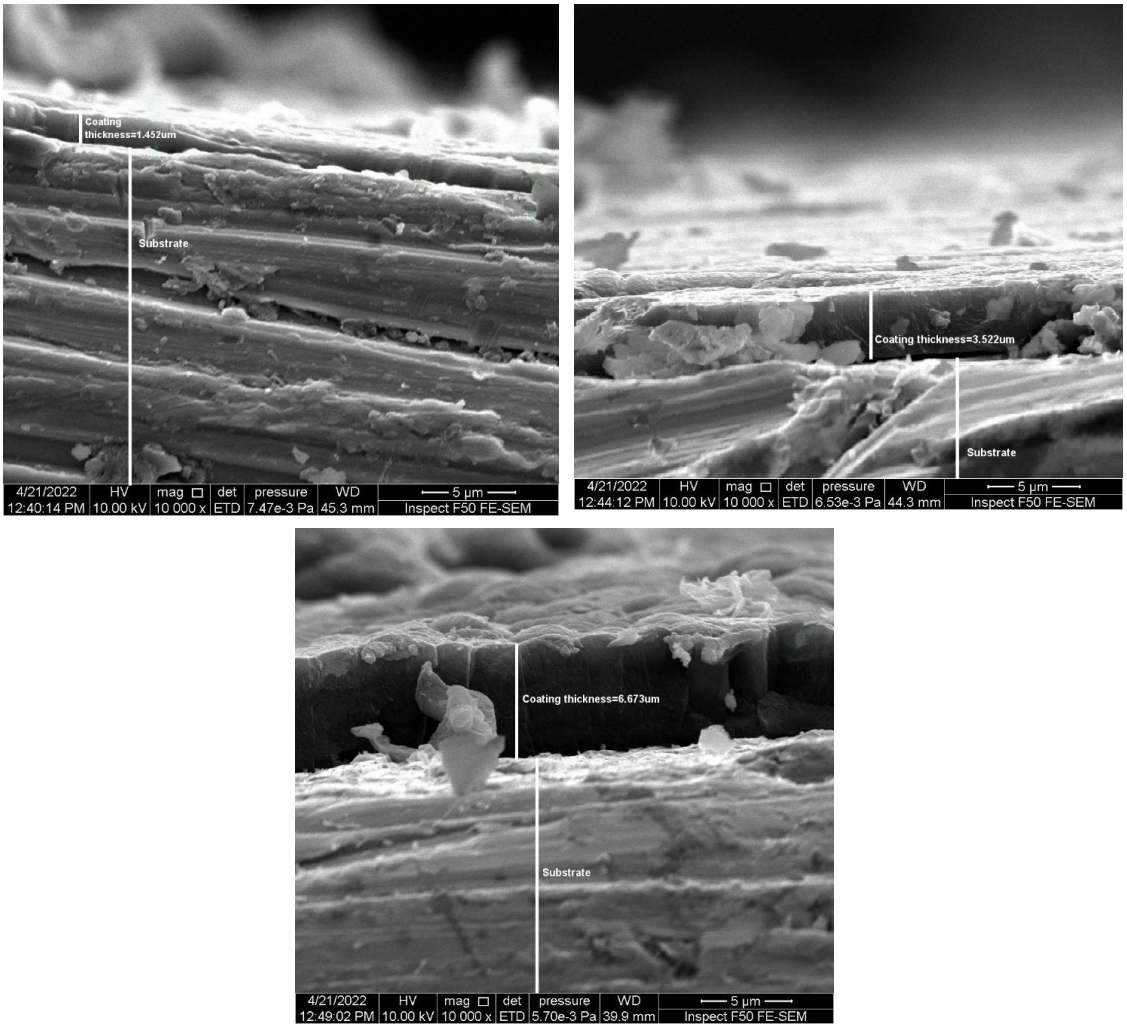

Fig. 3. FE-SEM images of the cross section of the coated samples: (a) 2-hour NbC deposited thin film at a magnification of 10,000x, (b) 4-hour NbC deposited thin film at a magnification of 10,000x, and (c) 6-hour NbC deposited thin film at a magnification of 10,000x.

nanometric range, as presented in (Table 2).

Contact angle measurement

The arithmetic mean of the measurements for the four variables is shown in (Table 3). Comparing the coated samples to the untreated Ti-6Al-7Nb alloy, the coated samples display reduced water contact angles.

Phase analysis

Various phases of niobium carbide were formed, including cubic NbC, orthorhombic Nb_2C, and monoclinic Nb_6C_5. It is not possible to achieve a phase-pure niobium carbide coating using the glow discharge process. Attempts were made to control the C_2H_2 and argon gas pressures inside the chamber to produce a phase-pure NbC coating. However, due to the need to maintain a constant pressure of $6*10^{-2}$ mBar, there was limited freedom to manipulate the gas pressure. The deposition process variables, such as plasma intensity and ion bombardment, can influence the composition and configuration of the coating material; comparable results have been validated by other studies [24,25].

The non-equilibrium conditions during sputter deposition result in a nanocomposite

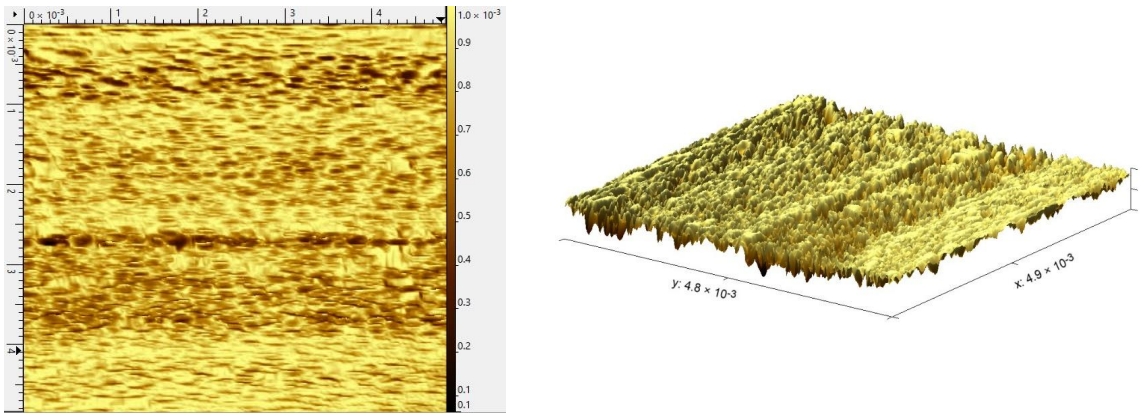

Fig. 4. AFM images illustrating the surface morphology of the uncoated Ti-6Al-7Nb samples. (a) displays the 2D image, while (b) depicts the corresponding 3D image.

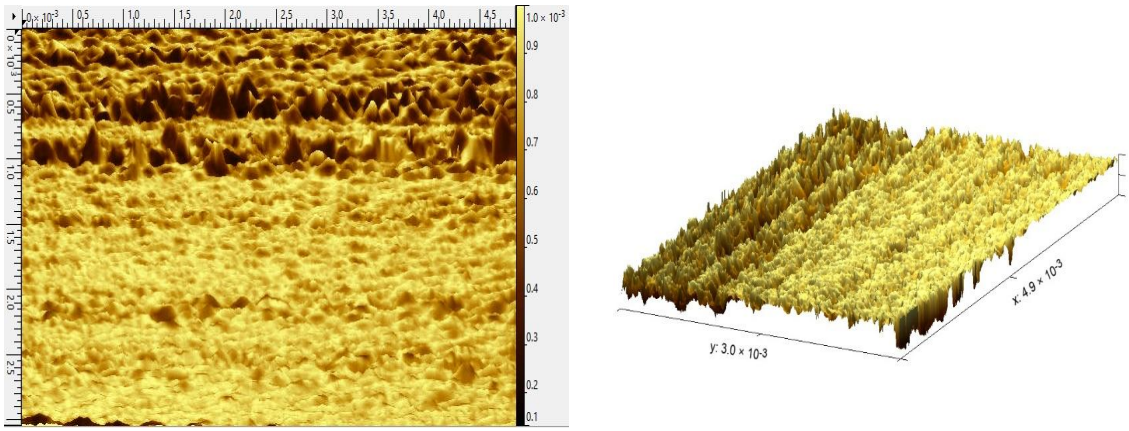

Fig. 5. AFM images illustrating the surface morphology of the 2-hour NbC coated Ti-6Al-7Nb samples produced under glow discharge. (a) presents the 2D image, while (b) presents the corresponding 3D image.

structure composed of nanocrystalline and often substoichiometric niobium carbide phases, along with an amorphous carbon phase [26]. The structure consists of nanometer-sized crystalline regions separated by seemingly disorganized regions of substoichiometric NbC phases, with the presence of a non-crystalline graphite phase (nanoclusters of NbC in amorphous carbon), which is consistent with earlier research [25,27].

It is important to note that the crystal structure of the phases is affected by the deposition time. The intensity of the niobium carbide XRD peaks decreases as the deposition time increases, with the NbC and Nb_2C being more affected; indicating a reduction in the crystallinity of the formed coating as the content of amorphous carbon increases with longer deposition times.

Microstructure

The morphology displayed is that of tiny particulates (on the nanometric scale) that agglomerate in a random manner to form clusters (or grains) as a result of the growth of coalesced nuclei (on the micrometric scale), which becomes more pronounced and intense as they approach the peaks of the finishing scratches.

The SEM image of the 2 hours deposited NbC film (Fig. 2a) shows larger agglomerates with high lightening regions of various pore sizes, attributed to niobium carbide; such a microstructure is suggestive of smaller crystal sizes and attracted particulates [28]. On (Fig. 2b and 2c), microstructural changes were detected as sputtering time was increased, explaining the continuous increase in grain size as sputtering

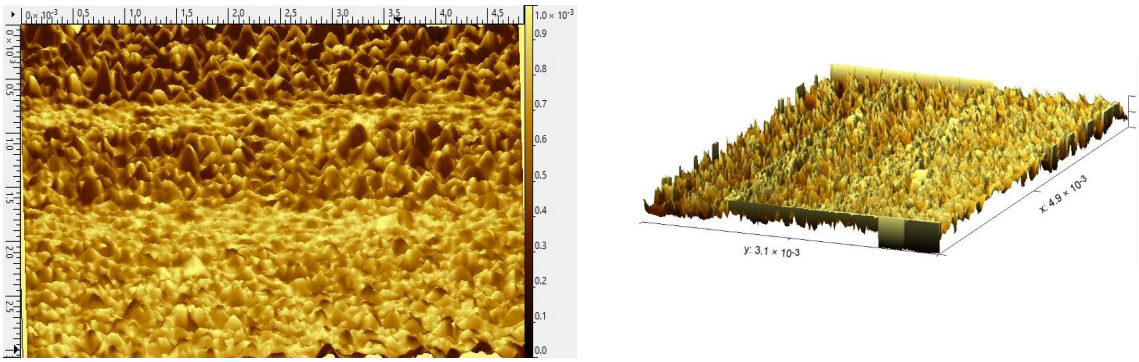

Fig. 6. AFM images depicting the surface morphology of Ti-6Al-7Nb coated with NbC for a deposition time of 4 hours using glow discharge. (a) 2D image and (b) 3D image.

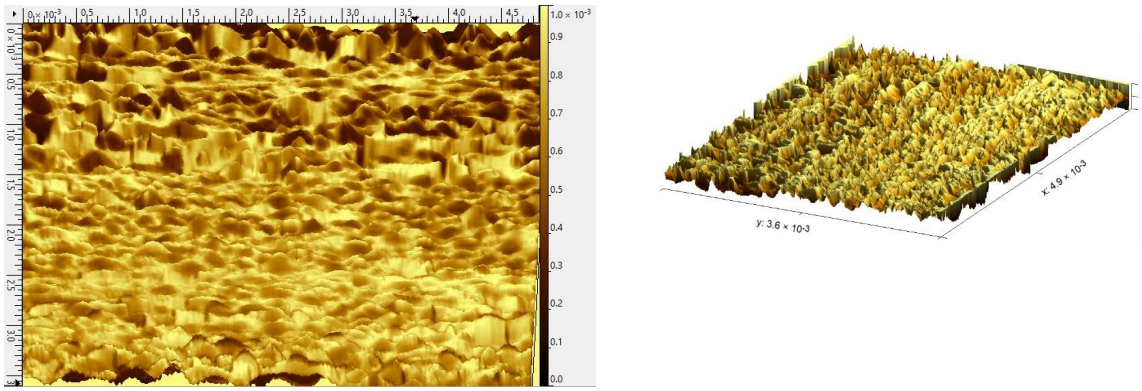

Fig. 7. AFM images displaying the surface morphology of Ti-6Al-7Nb coated with NbC for a deposition time of 6 hours using glow discharge. (a) is the 2D representation and (b) a 3D representation of the surface topography.

time was increased.

According to the data at hand, for the 2-hour deposition time, the average grain size is 0.914 µm. It increases to 1.33 µm for the 4-hour deposition time and further to 1.912 µm for the 6-hour deposition time, SEM images confirm these findings. As the grains grow larger, they start to join together and fuse. Grain size is a significant microstructural parameter in these materials, its significance arises from its role, along with its relative phase analysis facilitates the predictions regarding the structural configuration of the carbide layer and the grains separation [29].

Roughness analysis

The non-coated discs exhibit roughness (R_a: 118.9 nm) attributed to the manufacturing and polishing process (Fig. 4). The coated samples (Figs. 5, 6, and 7) display a more prominent and rougher surface with more apparent projections. The roughness values for the 2-hour group, 4-hour group, and 6-hour group are higher (R_a: 143.5 nm, 154.2 nm, and 152.4 nm, respectively).

Surface roughness increases with longer deposition time, as seen in AFM images. An explanation of such an increase in surface roughness may be given on the basis that the sputtered NbC particulates tend to be deposited and hit the topography of the substrate surface forming nuclei of agglomeration giving rise for larger grains and increasing the surface roughness[30], the deposition include the peaks and protrusions of the surface and be directed downhill to accumulate in the valleys and grooves of the substrates surface topography; similar results have been confirmed in a non-reactive process using high plasma density near the substrate [31].

In the 4-hour deposition time (Fig. 6), the surface exhibited a mean roughness (R_a) of 154.2 nm. However, in the subsequent 6-hour deposition time (Fig. 7), we observed a slight reduction in surface roughness, with Ra decreasing to 152.4 nm. Despite this reduction, it's important to note that the surface remained rougher compared to the control surface. This slight decrease in surface roughness can be attributed to the filling and bridging of finishing grooves and scratches by the sputtered NbC, resulting in surface smoothing as the deposition time increased [32].

Wettability

The wettability of a surface, whether it is hydrophilic or hydrophobic, can be determined by measuring the contact angle. A drop in water contact angle value from about 63° for the untreated Ti-6Al-7Nb surface to about 44° for the coated samples displays the production of more hydrophilic surface by the deposition of niobium carbide thin film (Table 3). The chemical composition of the NbC surface and its specific surface energy may explain the difference in wettability making the NbC film exhibit stronger wetting affinity compared to the uncoated

Table 2. Results of AFM measurements (R_a and R_q) of the NbC coated Ti-6Al-7Nb.

Surface parameter	Uncoated	2hrs	4hrs	6hrs
R_a (nm)	118.9	143.5	154.2	152.4
SD	3.557	4.666	4.451	6.526
SE	1.591	2.087	1.990	2.919
R_q (nm)	146.3	179.5	186.9	188.8
SD	3.798	4.524	4.693	4.804
SE	1.699	2.023	2.099	2.148

* R_a: Mean roughness.
* R_q: Root mean square of the height values of all points of a 3D scan.
*SD: Standard Deviation.
*SE: Standard Error.

Table 3. Results of the water contact angle measurements of the NbC coated Ti-6Al-7Nb.

	Uncoated Ti-6Al-7Nb	2hrs coating	4hrs coating	6hrs coating
Water contact angle (◦)	62.83	44.4	43.07	44.27
SD	4.307	3.890	2.420	4.044
SE	1.926	1.740	1.082	1.808

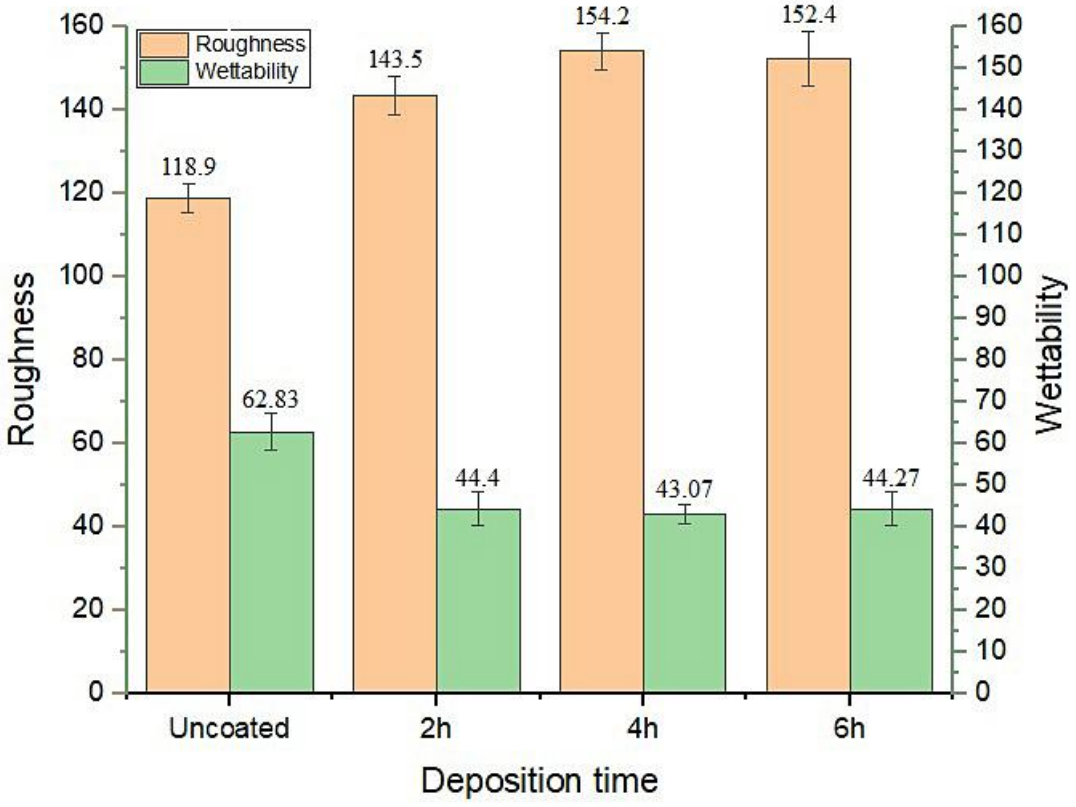

Fig. 8. Bar chart illustrating the relationship between surface roughness and water contact angle measurements for each specimen, including the uncoated sample, as well as the samples deposited for 2 hours, 4 hours, and 6 hours. The vertical lines on the chart represent the standard deviation.

titanium alloy samples [33].

The relationship between roughness and wettability values of the samples is displayed in (Fig. 8). The NbC coating increases the surface roughness of the titanium alloy samples compared to the uncoated samples, and simultaneously reduces the measured contact angle. This outcome is in agreement with the results of Gittens et al. [34] and Rupp et al. [35] According to the Wenzel theory; an essential theory of roughness-induced wetting; a wetting liquid completely fills a rough surface topography, including all indentations and pores, an important outcome of this theory allows hydrophilic surfaces with contact angles below 90° to become more hydrophilic with increasing the surface roughness, the issue that may well explain the reduction in contact angle measurements with increasing the deposition time [36,37]. As mentioned earlier, the roughness values increase with longer deposition times, accompanied by a simultaneous reduction in contact angle measurements. The surface treatment in this study affects the surface topography and has a substantial impact on wettability, as demonstrated in (Fig. 8).

CONCLUSION

In this study, NbC films were produced on Ti-6Al-7Nb substrates using the low-temperature plasma glow discharge technique. To comprehensively analyze the characteristics of the deposited surface layer and compare the effects of different deposition periods on the coatings, it is crucial to consider phase composition, microstructure, surface morphology, and wettability, as these factors can significantly influence the suitability of the coatings as biomaterials. Despite efforts to verify the C_2H_2 and argon gas pressure inside the chamber to achieve a phase-pure NbC coating, it was not feasible to produce a sample with a

completely pure niobium carbide phase using the glow discharge process. Different phases of niobium carbide were formed, including cubic NbC, orthorhombic Nb_2C, and monoclinic Nb_6C_5. The thin films consist of nanometer-sized crystalline regions separated by seemingly disordered substoichiometric NbC phases, with a non-crystalline graphite phase (nanoclusters of NbC in amorphous carbon). The observed microstructure reveals the presence of tiny particles on the nanometric scale that randomly aggregate to form clusters or grains due to the coalescence of nuclei on the micrometric scale. These clusters become more prominent and pronounced as they approach the peaks of the finishing scratches.

The roughness of the non-coated discs (R_a: 118.9 nm) can be attributed to the manufacturing and polishing processes, as the samples were ground with 1000 grit SiC paper. In contrast, the coated samples exhibit a more pronounced and rougher surface with noticeable projections. Surface roughness measurements were higher in the 2-hour, 4-hour, and 6-hour groups. The deposition of the niobium carbide thin film resulted in a more hydrophilic surface, as evidenced by a drop in the water contact angle for the coated samples. Longer deposition times were found to increase the roughness values and decrease the contact angle measurements concurrently. The surface treatment applied in this study modified the surface topography and had a significant impact on surface wettability.

CONFLICT OF INTEREST

The authors declare that there is no conflict of interests regarding the publication of this manuscript.

REFERENCES

1. Hamad TI, Fatalla AA, Waheed AS, Azzawi ZGM, Cao Y-g, Song K. Biomechanical Evaluation of Nano-Zirconia Coatings on Ti-6Al-7Nb Implant Screws in Rabbit Tibias. Current Medical Science. 2018;38(3):530-537.
2. Recent Advances and Prospects in type Titanium Alloys for Dental Implants Applications. American Chemical Society (ACS).
3. Lakshmi G, Raman V, Rajendran N, Babi MAK, Arivuoli D. In vitro corrosion behaviour of plasma nitrided Ti–6Al–7Nb orthopaedic alloy in Hanks solution. Science and Technology of Advanced Materials. 2003;4(5):415-418.
4. Fonseca-García A, Pérez-Alvarez J, Barrera CC, Medina JC, Almaguer-Flores A, Sánchez RB, et al. The effect of simulated inflammatory conditions on the surface properties of titanium and stainless steel and their importance as biomaterials. Materials Science and Engineering: C. 2016;66:119-129.
5. Liang Y, Qin H, Mehra N, Zhu J, Yang Z, Doll GL, et al. Controllable hierarchical micro/nano patterns on biomaterial surfaces fabricated by ultrasonic nanocrystalline surface modification. Materials & Design. 2018;137:325-334.
6. Wang G, Wan Y, Ren B, Liu Z. Fabrication of an orderly micro/nanostructure on titanium surface and its effect on cell proliferation. Mater Lett. 2018;212:247-250.
7. Rupp F, Gittens RA, Scheideler L, Marmur A, Boyan BD, Schwartz Z, et al. A review on the wettability of dental implant surfaces I: Theoretical and experimental aspects. Acta Biomater. 2014;10(7):2894-2906.
8. Spriano S, Sarath Chandra V, Cochis A, Uberti F, Rimondini L, Bertone E, et al. How do wettability, zeta potential and hydroxylation degree affect the biological response of biomaterials? Materials Science and Engineering: C. 2017;74:542-555.
9. Arabnejad S, Burnett Johnston R, Pura JA, Singh B, Tanzer M, Pasini D. High-strength porous biomaterials for bone replacement: A strategy to assess the interplay between cell morphology, mechanical properties, bone ingrowth and manufacturing constraints. Acta Biomater. 2016;30:345-356.
10. Chen C, Zhang S-M, Lee I-S. Immobilizing bioactive molecules onto titanium implants to improve osseointegration. Surf Coat Technol. 2013;228:S312-S317.
11. Kyzioł K, Rajczyk J, Wolski K, Kyzioł A, Handke B, Kaczmarek Ł, et al. Dual-purpose surface functionalization of Ti-6Al-7Nb involving oxygen plasma treatment and Si-DLC or chitosan-based coatings. Materials Science and Engineering: C. 2021;121:111848.
12. de Sousa LMR, das Virgens Santana M, da Silva BP, Marques TO, Peña-Garcia RR, Hidalgo AA, et al. Surface modification of Ti6Al7Nb alloy by Al_2O_3 nanofilms and calcium phosphate coatings. Surf Coat Technol. 2023;456:129249.
13. Sobiecki JR, Wierzchoń T. Glow discharge assisted oxynitriding of the binary Ti6Al2Cr2Mo titanium alloy. Vacuum. 2005;79(3-4):203-208.
14. Qayyum A, Imran M, Khan M, Ahmad S, Shah AU. Spectroscopic Evaluation of Nitrogen Glow Discharge for the Surface Nitriding of Ti-6al-4v Alloy. Elsevier BV; 2023.
15. Czyrskafilemonowicz A, Buffat P, Lucki M, Moskalewicz T, Rakowski W, Wierzchon T. Transmission electron microscopy and atomic force microscopy characterisation of titanium-base alloys nitrided under glow discharge. Acta Mater. 2005;53(16):4367-4377.
16. Amriou T, Bouhafs B, Aourag H, Khelifa B, Bresson S, Mathieu C. FP-LAPW investigations of electronic structure and bonding mechanism of NbC and NbN compounds. Physica B: Condensed Matter. 2003;325:46-56.
17. Nedfors N, Tengstrand O, Lewin E, Furlan A, Eklund P, Hultman L, et al. Structural, mechanical and electrical-contact properties of nanocrystalline-NbC/amorphous-C coatings deposited by magnetron sputtering. Surf Coat Technol. 2011;206(2-3):354-359.
18. Xu Z, Yate L, Qiu Y, Aperador W, Coy E, Jiang B, et al. Potential of niobium-based thin films as a protective and osteogenic coating for dental implants: The role of the nonmetal elements. Materials Science and Engineering: C. 2019;96:166-175.
19. Braic M, Braic V, Balaceanu M, Vladescu A, Zoita CN, Titorencu I, et al. Preparation and characterization of biocompatible Nb–C coatings. Thin Solid Films.

2011;519(12):4064-4068.
20. Al Qaysi HT, Hamad TI, Al Zubaidy TL. Analysis of the surface hardness of niobium carbide coatings deposited on commercially pure titanium and Ti-6Al-7Nb alloy implant materials using the glow discharge plasma technique. (Humanities, social and applied sciences) Misan Journal of Academic Studies. 2023 Dec 30;22(48):264-269.
21. Wierzchoń T, Czarnowska E, Grzonka J, Sowińska A, Tarnowski M, Kamiński J, et al. Glow discharge assisted oxynitriding process of titanium for medical application. Appl Surf Sci. 2015;334:74-79.
22. Boyd AR, Rutledge L, Randolph LD, Meenan BJ. Strontium-substituted hydroxyapatite coatings deposited via a co-deposition sputter technique. Materials Science and Engineering: C. 2015;46:290-300.
23. Liu X, Chu P, Ding C. Surface modification of titanium, titanium alloys, and related materials for biomedical applications. Materials Science and Engineering: R: Reports. 2004;47(3-4):49-121.
24. Braic V, Balaceanu M, Braic M. Grazing incidence mirrors for EUV lithography. 2008 International Semiconductor Conference: IEEE; 2008. p. 267-270.
25. Jansson U, Lewin E. Sputter deposition of transition-metal carbide films — A critical review from a chemical perspective. Thin Solid Films. 2013;536:1-24.
26. Lewin E, Persson POÅ, Lattemann M, Stüber M, Gorgoi M, Sandell A, et al. On the origin of a third spectral component of C1s XPS-spectra for nc-TiC/a-C nanocomposite thin films. Surf Coat Technol. 2008;202(15):3563-3570.
27. Lewin E, Olsson E, André B, Joelsson T, Öberg Å, Wiklund U, et al. Industrialisation Study of Nanocomposite nc-TiC/a-C Coatings for Electrical Contact Applications. Plasma Processes and Polymers. 2009;6(S1).
28. Souto MVM, Araujo CPBd, Lima MJS, Borges FMM, Gomes UU, Souza CPd. Synthesis and Characterization of Niobium Carbide with Copper Addition Obtained Via Gas Solid Reaction. Materials Research. 2018;21(3).
29. Cai X, Xu Y. Microstructure, friction and wear of NbC coatings on a Fe substrate fabricated via an in situ reaction. Surf Coat Technol. 2017;322:202-210.
30. Refaat MM, Hamad TI. Evaluation of Mechanical and Histological Significance of Nano Hydroxyapatite and Nano Zirconium Oxide Coating on the Osseointegration of CP Ti Implants. Journal of Baghdad College of Dentistry. 2016;28(3):30-37.
31. Barker CM, Lewin E, Patscheider J. Modified high power impulse magnetron sputtering process for increased deposition rate of titanium. Journal of Vacuum Science & Technology A: Vacuum, Surfaces, and Films. 2013;31(6).
32. Sansone M, De Bonis A, Santagata A, Rau JV, Galasso A, Teghil R. Pulsed laser ablation and deposition of niobium carbide. Appl Surf Sci. 2016;374:112-116.
33. Yate L, Coy LE, Gregurec D, Aperador W, Moya SE, Wang G. Nb–C Nanocomposite Films with Enhanced Biocompatibility and Mechanical Properties for Hard-Tissue Implant Applications. ACS Applied Materials & Interfaces. 2015;7(11):6351-6358.
34. Gittens RA, Olivares-Navarrete R, Cheng A, Anderson DM, McLachlan T, Stephan I, et al. The roles of titanium surface micro/nanotopography and wettability on the differential response of human osteoblast lineage cells. Acta Biomater. 2013;9(4):6268-6277.
35. Rupp F, Scheideler L, Rehbein D, Axmann D, Geis-Gerstorfer J. Roughness induced dynamic changes of wettability of acid etched titanium implant modifications. Biomaterials. 2004;25(7-8):1429-1438.
36. Quéré D. Wetting and Roughness. Annual Review of Materials Research. 2008;38(1):71-99.
37. Wenzel RN. Resistance of Solid Surfaces to Wetting By Water. Industrial and Engineering Chemistry. 1936;28(8):988-994.